A Beam Switchyard for Parallel Operation of Multiple Beamlines at the SXFEL User Facility*

Si Chen,[1,†] Kaiqing Zhang,[1] Zheng Qi,[1] Tao Liu,[1] Chao Feng,[1] Haixiao Deng,[1] Bo Liu,[1] and Zhentang Zhao[1,‡]

[1]*Shanghai Advanced Research Institute, Chinese Academy of Sciences, Shanghai 201210, China*

As an important measure of improving the efficiency and usability of X-ray free electron laser facilities, parallel operation of multiple undulator lines realized by a beam switchyard has become a standard configuration in the recent built XFEL facilities. SXFEL-UF, the first soft X-ray free electron laser user facility in China, has finished construction and commissioning recently. The electron beams from the linac are separated and delivered alternately to the two parallel undulator beam lines through a beam switchyard. A stable and fast kicker magnet is used to achieve bunch-by-bunch separation. Optics measures are applied to mitigate the impact of various collective effects, such as coherent synchrotron radiation and micro-bunching instability, on the beam quality after passing through the deflection line of the beam switchyard. In this study, the comprehensive physical design of the beam switchyard is described and the latest results of its commissioning process are presented.

Keywords: X-ray free electron laser, beam switchyard, double bend achromat, coherent synchrotron radiation

chinaXiv:202302.00250v1

I. INTRODUCTION

With the rapid development of high-gain Free Electron Laser technology, X-ray Free Electron Laser (XFEL) facilities have emerged as a powerful infrastructure that supports various scientific fields including but not limited to the bioscience, material science, chemistry and physics[2]. To meet the growing demand from various users in different scientific communities, there have been several X-ray Free Electron Laser user facilities built world wide, including several hard X-ray FEL facilities[3–7] and several soft X-ray FEL facilities[8, 9].

XFEL facilities require extremely high-brightness electron beams with not only a small transverse emittance but also small energy spread and high peak current. Typically, high-performance RF linear accelerator is used to provide the high quality beam of an XFEL facility and thus its capacity of user beamlines is limited compared with those of the storage-ring based sychrotron radiation light sources. The growing number of users and their various photon parameter requirement naturally arises a demond of building more user beamlines with different configurations. As compared to the high cost of building a new XFEL facility, a more efficient and economical approach is to improve the beam utilization efficiency by distributing the beam to several separated undulator lines, which is realized by a *beam switchyard* (sometimes also referred as the *beam distribution system*). In the recent built XFEL facilities, beam switchyard is becoming a standard configuration in order to accommodate multiple undulator lines with various X-ray parameters for feeding more beamlines[13–17, 19]. In such a beam switchyard, electron bunches from linear accelerator are separated by switching magnets and delivered alternately to each undulator line on a predetermined model, either pulsed or bunch-by-bunch. At the mean time, the beam quality should be well maintained during the beam distribution process, especially when the beam current is high, which is usualy a necessary for high-gain XFEL.

Recent years, several XFEL facilities have been built or proposed in China. The Shanghai soft X-ray FEL (SXFEL) facility, as the first X-ray FEL facility in China, has started commissioning in 2021. A high repetition rate hard X-ray FEL facility, which is named as SHINE, has also started construction. Both of the facilities are designed to have multiple undulator beamlines. For the SXFEL facility, two undulator lines are driven by a normal conducting RF linac with 50 Hz bunch repetition rate, as is described in Section II. A beam switchyard is used between the linac and undulator section for simultaneous operation of the two undulator lines. In this paper, the physics design and start-to-end simulation result of the beam switchyard, with the consideration of suppressing beam collective effect such as the coherent synchrotron radiation (CSR) and micro-bunching instability (MBI), is descirbed in Section III. The commissioning results are presented in Section IV, followed by a summary in Section V.

II. THE SXFEL FACILITY

The SXFEL facility is aimed to open up the enormous field related to XFEL in China and to accumulate the indispensable technical experience for constructing and utilizing the future hard x-ray FEL facility. It is developed in phases. First a test facility (SXFEL-TF) with a $840\,\mathrm{MeV}$ linac is built for generation of $8.8\,\mathrm{nm}$ full coherent soft X-ray radiation and technical validation of various seeded FEL mechanisms. In 2020, it has achieved its goal with the demonstration of two-stage HGHG-HGHG cascade and two-stage EEHG-HGHG cascade schemes.

Soon afterwards, the SXFEL-TF has been upgraded and integrated to the user facility (SXFEL-UF)[11]. It is de-

* This work was supported by the National Key Research and Development Program of China (2018YFE0103100), the National Natural Science Foundation of China (12125508, 11935020), Program of Shanghai Academic/Technology Research Leader (21XD1404100), and Shanghai Pilot Program for Basic Research – Chinese Academy of Science, Shanghai Branch (JCYJ-SHFY-2021-010).

† chensi@zjlab.org.cn

‡ Corresponding author, zhaozhentang@zjlab.org.cn

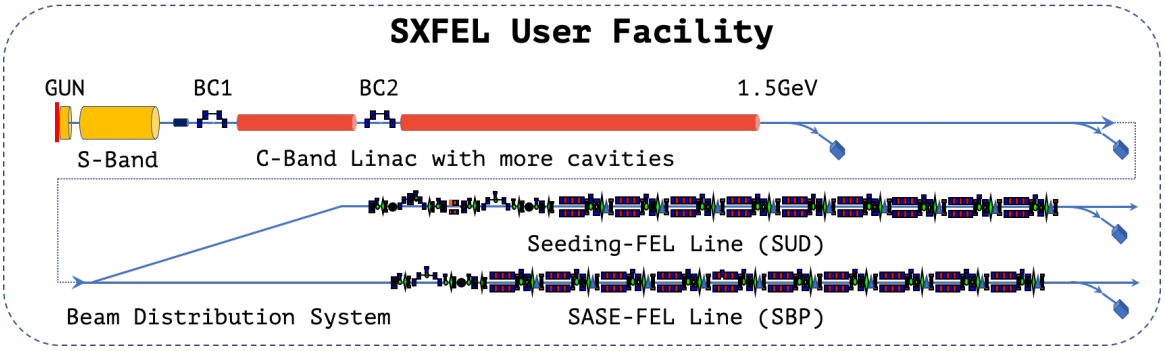

Fig. 1. Schematic view of the SXFEL-UF.

signed to cover the whole water window range. To accomplish this, the beam energy is upgraded to about 1.5 GeV by adding more C-band RF structures to the linac. Two individual undulator lines are parallelly installed in the newly built undulator hall. Directly downstream of the linac it is a brand new SASE-FEL line with radiation wavelength about 2 nm. The existing seeding-FEL line of SXFEL-TF is moved to about 3 m right side of the SASE-FEL line with an upgrade of more undulator sections for a radiation wavelength about 3 nm. The schematic layout of the SXFEL-UF is shown in Fig. 1. Some main beam parameters of SXFEL-UF are shown in Table 1.

Table 1. Main Parameters of SXFEL Linac

Parameters	Values	Units
E	1.5∼1.6	GeV
σ_E/E (rms)	≤0.1 %	
ε_n (rms)	≤1.5	mm·mrad
l_b (FWHM)	≤0.7	ps
Q	500	pC
I_{pk}	≥700	A
f_{rep}	50	Hz

For maximizing the operation efficiency of the facility, it is naturally expected that the two undulator lines can provide FEL radiation to multiple users simultaneously. As is seen in Fig. 1, for the parallel operation of the two FEL lines, a beam switchyard is located between the linac and undulator section. The 50 Hz electron bunch train from linac is distributed in two directions, either to the SASE-FEL line or to the seeding-FEL line. Because of the high requirement of the external seeded FEL, the beam switchyard should be able to guarantee a stable, precise transportation of the electron beam with a well maintained beam quality properties, such as the low emittance, high peak charge and short bunch length. In the following sections, the physics design and commissioning results of such a beam switchyard are described in detail.

III. BEAM SWITCHYARD DESIGN OF SXFEL-UF

A. General Layout

First step of the beam distribution is the separation of the bunch trains to different direction. The beam switchyard uses a fast switching kicker magnet with the ability of bunch-by-bunch distribution of the 50 Hz electron bunch train from the linac. It is also designed to be programmable for an arbitrary distribution pattern, which means the bunch frequency of each undulator line can be easily modified based on the requirement of user experiments. When the kicker magnet is trigged on, the electron bunch is deflected horizontally to the seeding-FEL line through a deflection switchyard, otherwise it goes straight to the SASE-FEL line directly downstream of the linac without any deflection.

Since the two FEL lines lie parallel in the undulator hall, the deflection line uses a dog-leg structure to bring the kicked beam to the entrance of the seeding-FEL line. Due to the limitation of the longitudinal distance, the total deflection angle of the dog-leg is about 6°. The most immediate effect of the dog-leg is the dispersion function. When electron bunch with non-zero energy spread passes through a bending magnet, dispersion effect introduces a coupling between the transverse position and the energy of each electron in the bunch so that the electrons spread transversely afterwards. The transverse phase space can be severely destroyed by this effect. In order to cancel the dispersion of beam distribution dog-leg, its entrance and exit bending magnets are replaced by two identical double-bend-achromat (DBA) sections, respectively. In such a configuration, both the dispersion element (R_{16}) and the dispersion divergence element (R_{26}) are cancelled locally after each DBA and globally after the whole dog-leg. The dispersion evolution along the dog-leg is shown in Fig. 3 as the dashed lines. Between the two DBA sections, several quadruples are inserted for beam matching. The position of the elements is adjusted carefully to avoid conflict between the straight line and the deflected line. The total projected length of the dog-leg is about 39 m. A schematic view of such a dog-leg is shown in Fig. 2.

chinaXiv:202302.00250v1

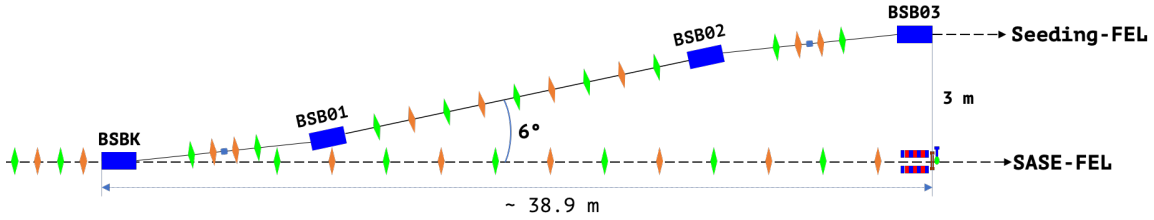

Fig. 2. Schematic layouts of the beam switchyard of SXFEL-UF. The total bending angle of the beam distribution dog-leg is about 6° with the limitation of total available space for beam switchyard. A pulsed kicker magnet acts as the first bending magnet of the dog-leg with the ability of bunch-by-bunch distribution between the two FEL lines.

chinaXiv:202302.00250v1

B. Optics Design for CSR & MBI Suppression

For high-gain XFEL facilities, typically a high peak current, low emittance electron beam is necessary for obtaining as higher gain in as shorter gain length. However, when such a intense electron beam passes through the deflection line of the beam switchyard, several kinds beam collective effect, such as the emittance growth induced by coherent synchrotron radiation, and the micro-bunching instability, may spoil both the transverse and longitudinal phase space of the electron beam, and in further reduces the performance of x-ray free electron laser. To avoid this,it is necessary to consider the suppression of beam collective effects of intense electron beam passing through the deflection switchyard in the optics design.

Coherent synchrotron radiation (CSR) introduced emittance growth is one of the critical beam dynamic issues of the beam distribution dog-leg. When the electron bunch passes through the bending magnet, synchrotron radiation is emitted. If the bunch length is short enough that it is comparable with the radiation spectral components, the synchrotron radiation becomes coherent. CSR from the bunch tail part may catch up with the head part and interact with the electrons inside as the bunch goes by. Both the transverse and longitudinal phase space distribution can be changed by this process. In longitudinal direction, the CSR field introduces a energy modulation along the longitudinal coordinate of the bunch so that the energy spread increases. In transverse direction, the CSR field mainly acts as a special term of dispersion due to the longitudinal energy variation ans thus the emittance in the bending direction grows. The growth of the projected emittance due to the CSR effect can be estimated as:

$$\frac{\Delta\varepsilon}{\varepsilon_0} \simeq \frac{1}{2}\frac{\beta}{\varepsilon_0}\theta^2\sigma^2_{\delta,CSR} \tag{1}$$

where β is the transverse twiss function at the bending magnet, θ is the deflection angle, and $\sigma_{\delta,CSR}$ is the CSR induced emittance growth, which is expressed as[18]:

$$\sigma_{\delta,CSR} = 0.2459 r_e \frac{N}{\sqrt[3]{R^2\sigma_z^4}}\frac{R\theta}{\gamma} \tag{2}$$

where r_e is the electron radius, N is the electron population of the bunch, R is the bending radius, and σ_z the RMS bunch length.

Eq.1 indicates that it is necessary and possible to suppress or even cancel the CSR induced emittance growth by well designed beam optics in an achromatic bending structure such as the beam distribution switchyard of SXFEL-UF. According to the proportional relation between the emittance growth and the β function on the bending plane of the bending magnet, the first approach of suppressing the emittance growth is simply by matching the beam envelope at the bending magnet to be a small beam waist. Another approach is by matching the lattice of switchyard dog-leg to be mirror symmetrical, and adjust the betatron phase advance between the two achromat to be an odd multiple of π, which is so called "optics balance" method[19]. With this approach, the CSR induced longitudinal dispersion and transverse kick are canceled at the exit of dog-leg. For the beam distribution switchyard of SXFEL-UF, a lattice design for mitigation the CSR emittance growth is shown in Fig. 3.

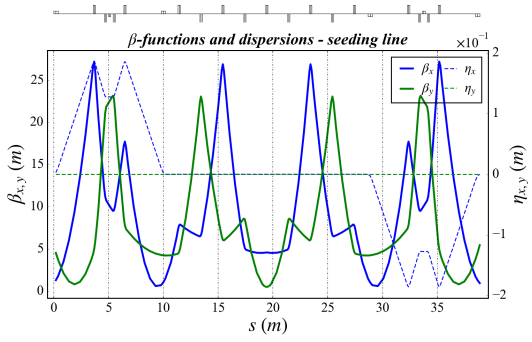

Fig. 3. Twiss functions ($\beta_{x,y}$) and dispersion functions ($\eta_{x,y}$) evolution along the dog-leg. The β_x at the entrance kicker magnet is optimize to be around 1.6 m so that all the bending magnets have the similar value with the symmetrical optics. The maximum values of β and $|\eta|$ are also optimized for smaller beam stay-clear area.

Another critical beam dynamic issue of the beam switchyard is the micro-bunching instability (MBI). It results from an interplay of various collective effects such as longitudinal space charge (LSC) effect, coher-

chinaXiv:202302.00250v1

ent synchrotron radiation (CSR) in dipole magnets, and the energy-dispersion correlation in magnetic bunch length compressors. An energy modulation is introduced in the beam longitudinal phase space and it is easily being converted to a density modulation while passing through a dispersive magnetic optics section with non-zero R_{56}. The amplified density modulation further drives even larger energy and density modulations downstream, thus the beam quality is significantly downgraded. Micro-bunching gain should be well suppressed in the beam switchyard with multi-bend deflection line to guarantee a high spectral brilliance, especially at output radiation wavelengths in EUV and soft x-ray range. For this purpose, a small bending magnet (micro-bend) is inserted in the middle of the DBA cell with a small angle reverse to the DBA deflection angle. With this design, the R_{56} of each DBA becomes zero. Apply this design to both of the DBA cells of the switchyard, it becomes globally isochronous, as is shown in Fig. 4. With the isochronous configuration, the deflection line of the beam switchyard is substantially transparent to any incoming modulation induced by micro-bunching instability in the linac.

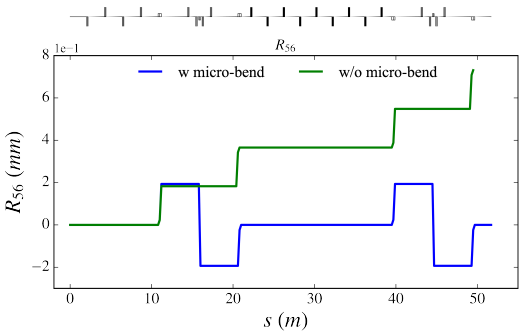

Fig. 4. R_{56} evolution along the dog-leg. Without micro-bend, the global R_{56} is over 700 μm while with the micro-bend, the R_{56} is eliminated to less than 1 μm, which is negligible for micro-bunching growth.

C. S2E Tracking Results

The start-to-end tracking from the linac end throughout the beam distribution section is performed by the code ELEGANT[20]. The longitudinal phase space at the linac exit is shown in Fig. 5. Two stage compression bring the 500 pC electron bunch from 10 ps after the injector to less than 0.7 ps at the exit of linac with a long flat top in the longitudinal phase space, which is necessary for multi-stage energy modulation in some complex seeding-FEL mechanisms. Laser heater is used for smoothing the longitudinal phase space and a slice energy spread of about 1×10^{-4} is obtained at last. The peak current on the flat top part is about 800 A and the normalized emittance is about 1.0 $mm \cdot mrad$.

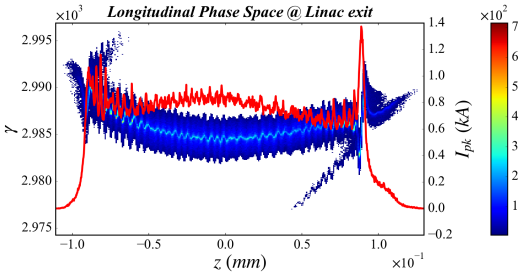

Fig. 5. Longitudinal phase space at the linac exit. Beam central energy is about 1.5 GeV, bunch length (FWHM) is about 700 fs, peak current is about 800 A on the flat top and the normalized emittance is about 1.0 mm· mrad.

Fig. 6 shows the normalized emittance growth $(\varepsilon_{x,f}/\varepsilon_{x,o})$ with respect to the betatron phase advance (ϕ) between the two DBA cells, where the f and o denoted in the subscripts indicate the values at the end of linac and the beam distribution dog-leg respectively. It is clear that the emittance growth is almost completely eliminated with the π phase advance, which indicates that the current optics well satisfies the requirement of suppressing the CSR introduced emittance growth.

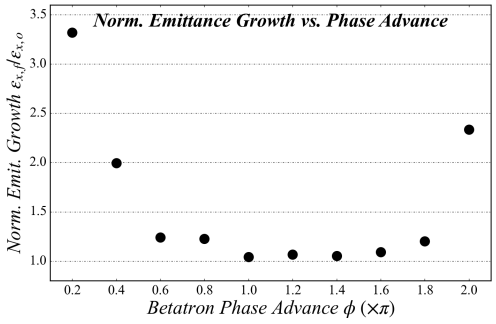

Fig. 6. Normalized emittance growth with respect to the betatron phase advance between the two DBA cells. Minimum emittance growth appears at $\phi \sim \pi$, which is much less than the expected 10 %.

As is seen in Fig. 5, although the laser-heater is used, some residual micro-bunching structures still appear in the longitudinal phase space. Besides, there is a horn with peak current over 1.5 kA in the bunch head part. A comparison of the t-x phase space and current profile before and after the switchyard is shown in Fig. 7. For the case that $R_{56} \neq 0$, it shows an obvious growth of the microbunching structure in the longitudinal phase space, especially on the head horn part. For the isochronous case with micro-bend, only imperceptible microbunching gain can be observed. The longitudinal phase space is well preserved after the distribution dog-leg.

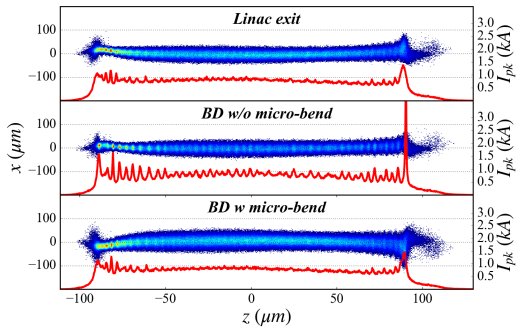

Fig. 7. Comparison of the t-x phase space and the current profile at linac exit (upper), BD exit without micro-bend (middle) and BD exit with micro-bend (lower).

D. Trajectory Stability

For sufficient and stable interaction between beam and seed laser, the seeded FEL line requires a transverse beam position jitter less than $0.1\sigma_x$. The major sources of the horizontal trajectory jitter come from the magnet power fluctuation especially the kicker magnet power jitter. The vertical jitter mainly comes from the quadrupole misalignment jitter due to ground vibration.

A simulation of the trajectory jitter of the beam switchyard is done with the kicker power jitter $\sim$ 100 ppm, bending magnet power jitter $\sim$ 50 ppm and ground vibration amplitude $\sim 200\,\mathrm{nm}$ in both horizontal and vertical direction (all in RMS). Fig. 8 shows the transverse trajectory jitter along the beam distribution dog-leg of 200 random seeds of the jitter source. The horizontal position jitter (RMS) at the exit of dog-leg is less than $0.1\sigma_x$ and the vertical position jitter (RMS) is less than $1\,\%$ of σ_y. However, a further simulation shows that the trajectory jitter is dominated by the kicker jitter and grows almost linearly with it. In a word, 100 ppm is the criteria amplitude of the acceptable kicker power jitter.

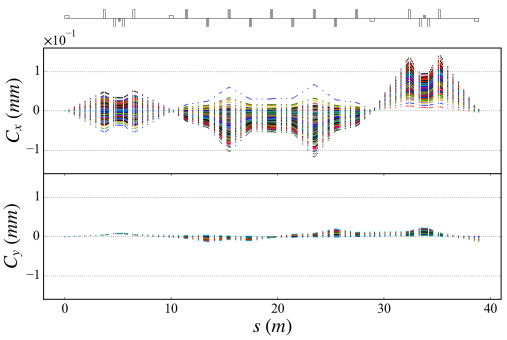

Fig. 8. Transverse trajectory jitter of 200 cases of jitter source. The horizontal trajectory jitter is less than $10\,\%$ with respect to the beam size σ_x and $<1\,\%$ in vertical direction

IV. COMMISSIONING RESULTS

A. Commissioning of the Deflection Line

The beam switchyard of SXFEL-UF has been installed in the front part of the newly built undulator hall in late 2020. The commissioning of the Switchyard and Seeding FEL line has started at the beginning of November 2021. However, since the power supply of the kicker magnet hasn't reach the expected stability requirement, as is described in the upper section, it is not acceptable for stable operation of seeding-FEL line. So the kicker magnet is absent in this stage of commissioning until it is stable enough and it's function is instead of a DC bending magnet temporary.

The dispersion function measurement is based on measuring the orbit change at each cavity BPM with different beam energy. As is seen in Eq. 3, if the dispersion is closed, the orbit data will not change with the energy change, otherwise there will be an orbit vs. relative energy change slope observed. By fitting the slope the dispersion function and even higher order dispersion terms can be obtained.

$$x = x_0 + R_{16}\frac{\Delta E}{E} + T_{166}(\frac{\Delta E}{E})^2 + ... \qquad (3)$$

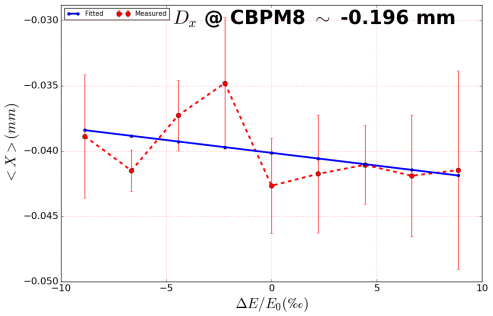

Fig. 9. The transverse dispersion is measured by monitoring the position variation on CBPM while varying the bending angle as an equivalence of varying beam energy.

Fig. 9 shows the measurement result of horizontal dispersion at the exit of distribution dog-leg. The residual horizontal dispersion after the dog-leg is cancelled to less than $1\,\mathrm{mm}$ which is much smaller than the required $10\,\mathrm{mm}$ value. In order to make sure the η_x' is also also well cancelled, dispersion is measured at more CBPMs downstream. Fig. 10 shows the measured dispersion at all the CBPMs from the beam switchyard to the entrance of the FEL line as a comparison with the theoretical value. The result not only confirms the reliability of measurement but also confirms a well cancellation of η_x'.

The betatron matching of beam switchyard is done by keeping the theoretical configuration of magnets while matching the entrance parameter from the linac. The emittance and twiss parameters are measured by varying the

chinaXiv:202302.00250v1

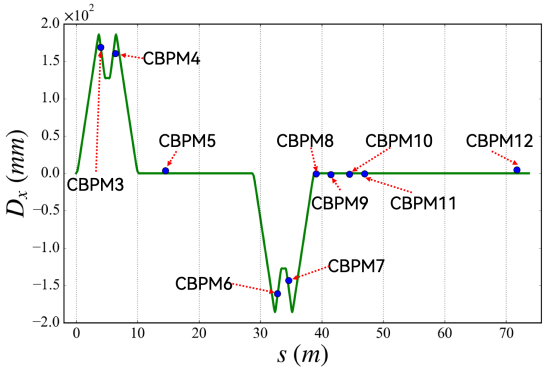

Fig. 10. The dispersion is measured on all the CBPMs along and downstream the beam distribution line and the data shows a good consistency with the theoretical value.

quadrupole and fitting the beam spot variation on a downstream OTR screen. Then the beam is matched from linac exit to the entrance of beam switchyard by an automatic algorism based on the code *Ocelot*. Fig. 11 shows the comparison between the observed beam spot on each screen and the theoretical beam spot after matching, which shows a well agreement. With such an optics, the emittance is measured after the dog-leg. In order to reduce the fluctuation of emittance measurement, an average of multi-times measurement has been down and the result shows a emittance growth only about 3 %, which is well below the requested 10 % emittance growth.

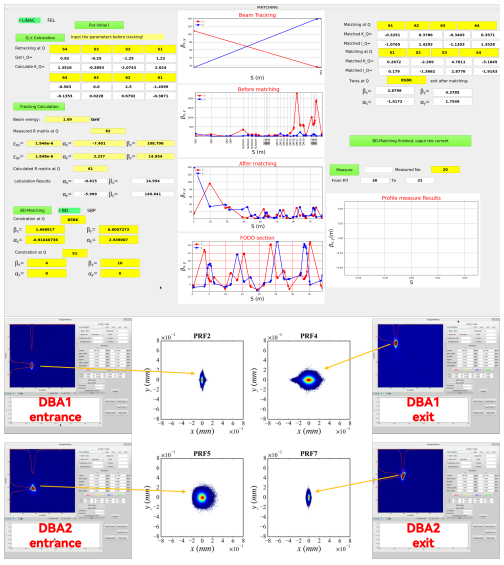

Fig. 11. The beam spot at each beam profile monitor as a comparison with the theoretical beam spot. With the well cancelled CSR induced emittance growth, the beam envelop is well sustained along the beam distribution line.

B. Parallel Operation of the Two Lines

The kicker magnet has been installed online in middle of 2022, with its field stability reaching the required criteria. This enables the simultaneous commissioning and operation of the two undulator lines. Fig.12 shows the installed kicker magnet and its high stability pulsed power supply in the undulator tunnel.

Fig. 12. Kicker magnet and its high stability pulsed power supply installed in the undulator tunnel.

A comparison of the transverse position jitter before and after the dog-leg is shown in Fig. 13. With the high stability kicker magnet, combined with the well canceled dispersion and CSR emittance growth in the deflection line, the growth of transverse position jitter after the dog-leg is less than 10 %. Soon afterward, a simultaneous lasing of the two undulator lines has been realized, as is seen in Fig. 14. This demonstrates the final success of the design and commissioning of the beam switchyard of SXFEL-UF.

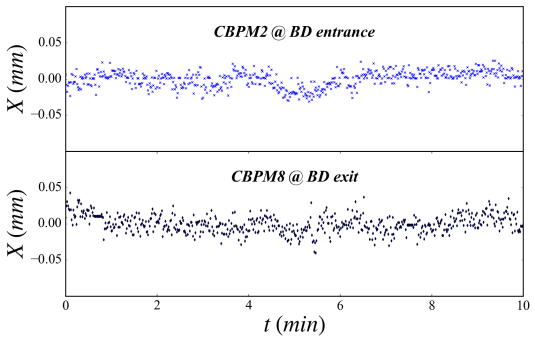

Fig. 13. A comparison of the transverse beam central position jitter between the entrance and exit of the BD section. Only imperceptible micro-bunching structure is observed.

chinaXiv:202302.00250v1

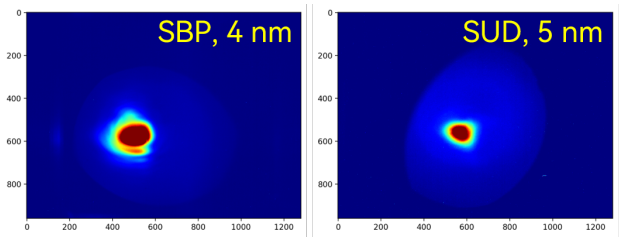

Fig. 14. Longitudinal phase space distribution of the electron beam after BD section.

V. SUMMARY

A beam switchyard of SXFEL-UF is designed to perform a bunch-by-bunch separation of the 50 Hz electron beam to the two undulator lines respectively. With properly optimized optics, some beam collective effects that may spoil the beam quality can be well suppressed. The beam distribution has been installed in the undulator tunnel and started commissioning in Nov. 2021. The commissioning results show that the beam quality after passing through the beam switchyard is well preserved with the present design. The electron beam passes through the beam distribution has been delivered to the downstream FEL line and an exponential FEL power growth has been obtained, which indicates the beam quality after the beam switchyard well satisfies the requirement of soft X-ray FEL. With the kicker magnet satisfies the stability requirement, simultaneous operation and lasing of the two undulator lines has been realized. The efficiency of the SXFEL-UF is significantly improved by the beam switchyard. And beyond that, it provides an important reference to the beam switchyard of the future hard X-ray free electron laser facility.

VI. ACKNOWLEDGMENT

The author would like to thank all the colleagues working on the SXFEL-UF. Special thanks to Duan Gu and Zhen Wang for providing the electron distributions used for this study. Many useful discussions with Bart Fattz and other members of the physics and commissioning team are also gratefully acknowledged.

chinaXiv:202302.00250v1

[1] Z.T. Zhao. Storage Ring Light Sources. Reviews of Accelerator Science and Technology. Vol. 03, No. 01, pp. 57-76 (2010). DOI:10.1142/S1793626810000361

[2] N. Huang, H.X. Deng, B. Liu et al., Features and Futures of X-ray Free-Electron Lasers. The Innovation. 2(2), 100097. DOI:10.1016/j.xinn.2021.100097

[3] P. Emma, R. Akre, J. Arthur et al. First lasing and operation of an ångstrom-wavelength free-electron laser. Nature Photon 4, 641–647 (2010). DOI:10.1038/nphoton.2010.176

[4] T. Ishikawa, H. Aoyagi, T. Asaka et al. A compact X-ray free-electron laser emitting in the sub-ångström region. Nature Photon 6, 540–544 (2012). DOI:10.1038/nphoton.2012.141

[5] H.S. Kang, C.K. Min, H. Heo et al. Hard X-ray free-electron laser with femtosecond-scale timing jitter. Nature Photon 11, 708–713 (2017). DOI:10.1038/s41566-017-0029-8

[6] E. Prat, R. Abela, M. Aiba et al. A compact and cost-effective hard X-ray free-electron laser driven by a high-brightness and low-energy electron beam. Nature Photonics 14, 748–754 (2020). DOI:10.1038/s41566-020-00712-8

[7] W. Decking, S. Abeghyan, P. Abramian et al. A MHz-repetition-rate hard X-ray free-electron laser driven by a superconducting linear accelerator. Nature Photonics 14, 391–397 (2020). DOI:10.1038/s41566-020-0607-z

[8] W. Ackermann, G. Asova, V. Ayvazyan et al. Operation of a free-electron laser from the extreme ultraviolet to the water window. Nature Photon 1, 336–342 (2007). DOI:10.1038/nphoton.2007.76

[9] E. Allaria, R. Appio, L. Badano et al. Highly coherent and stable pulses from the FERMI seeded free-electron laser in the extreme ultraviolet. Nature Photon 6, 699–704 (2012). DOI:10.1038/nphoton.2012.233

[10] Z.T. Zhao, D. Wang, Q. Gu et al., SXFEL: A Soft X-ray Free Electron Laser in China. Synchrotron Radiation News, Vol.30(2017) 6, pp.29-33. DOI:10.1080/08940886.2017.1386997

[11] B. Liu,, C. Feng, D. Gu et al., The SXFEL Upgrade: From Test Facility to User Facility. Appl. Sci. 2022,12,176. DOI:10.3390/app12010176

[12] Z.T. Zhao, D. Wang, Z.H. Yang et al., "SCLF: An 8-GeV CW SCRF Linac-Based X-Ray FEL Facility in Shanghai", in Proc. 38th Int. Free Electron Laser Conf. (FEL'17), Santa Fe, NM, USA, Aug. 2017, paper MOP055, pp. 182-184, ISBN: 978-3-95450-179-3, DOI:10.18429/JACoW-FEL2017-MOP055, 2018.

[13] T. Hara, K. Fukami, T. Inagaki et al., Pulse-by-pulse multi-beam-line operation for x-ray free-electron lasers. Phys. Rev. Accel. Beams 19, 020703 (2016). DOI:10.1103/PhysRevAccelBeams.19.020703

[14] T. Hara, C. Kondo, T. Inagaki et al., High peak current operation of x-ray free-electron laser multiple beam lines by suppressing coherent synchrotron radiation effects. Phys. Rev. Accel. Beams 21, 040701 (2018). DOI:10.1103/PhysRevAccelBeams.21.040701

[15] Y. Nosochkov, P. Emma, T. Raubenheimer et al., Development of the LCLS-II Optics Design. in Proceedings of IPAC2016, Busan, Korea, MOPOW048. DOI:10.18429/JACOW-IPAC2016-MOPOW048

[16] N. Golubeva, V. Balandin, W. Decking, Optics for the Beam Switchyard at the European XFEL. in Proceedings of IPAC2011, San Sebastián, Spain, WEPC008.

[17] N. Milas and S. Reiche, Switchyard Design: ATHOS, in Proceedings of FEL2012, Nara, Japan, MOPD37.

[18] M. Borland, Simple method for particle tracking with coherent synchrotron radiation. Phys. Rev. S.T. - Accel. Beams 4, 070701 (2001). DOI: 10.1103/PhysRevSTAB.4.070701

[19] S. Di Mitri, M. Cornacchia, and S. Spampinati, Cancellation of Coherent Synchrotron Radiation Kicks with

Optics Balance. Phys. Rev. Lett. 110, 014801 (2013). DOI:10.1103/PhysRevLett.110.014801

[20] M. Borland, elegant: A Flexible SDDS-Compliant Code for Accelerator Simulation, Advanced Photon Source LS-287, September 2000.

chinaXiv:202302.00250v1